TU Delft

Delft University of Technology

Document Version
Final published version

Licence
Other

Citation (APA)
Wuite, G., Tenpierik, M., & Lugten, M. (2023). Determining causes of variance in ground-level aircraft noise: Combining in-situ noise and weather measurements with spatial aircraft data. In A. Astolfi, F. Asdrubali, & L. Shtrepi (Eds.), *Proceedings of Forum Acusticum 2023: 10th Convention of EAA* (pp. 5481-5488). Politecnico di Torino. https://doi.org/10.61782/fa.2023.0438

Important note
To cite this publication, please use the final published version (if applicable).
Please check the document version above.

Copyright
In case the licence states “Dutch Copyright Act (Article 25fa)”, this publication was made available Green Open Access via the TU Delft Institutional Repository pursuant to Dutch Copyright Act (Article 25fa, the Taverne amendment). This provision does not affect copyright ownership.
Unless copyright is transferred by contract or statute, it remains with the copyright holder.

Sharing and reuse
Other than for strictly personal use, it is not permitted to download, forward or distribute the text or part of it, without the consent of the author(s) and/or copyright holder(s), unless the work is under an open content license such as Creative Commons.

Takedown policy
Please contact us and provide details if you believe this document breaches copyrights.
We will remove access to the work immediately and investigate your claim.

This work is downloaded from Delft University of Technology.

DOI: 10.61782/fa.2023.0438

forum acusticum 2023

DETERMINING CAUSES OF VARIANCE IN GROUND-LEVEL AIRCRAFT NOISE: COMBINING IN-SITU NOISE AND WEATHER MEASUREMENTS WITH SPATIAL AIRCRAFT DATA

Gustaf Wuite[1,2*] **Martijn Lugten**[1,2] **Martin Tenpierik**[1]
[1]Department of Architectural Engineering and Technology, TU Delft, Netherlands
[2] Amsterdam Institute for Metropolitan Solutions, Amsterdam, Netherlands

ABSTRACT

Aircraft are a source of noise pollution in areas surrounding airports. Buildings shield or amplify local sound levels, albeit that the level of shielding varies considerably. The sound pressure levels reaching ground receivers in the built environment depend on flight position relative to the receiver, atmospheric and weather effects, and the composition of the surrounding buildings. Their combined effect on local ground sound levels and noise shielding remains unclear however.

The impact of urban and architectural design on the local attenuation of aircraft noise is studied in a full-scale field lab near Amsterdam Schiphol airport. In the experiment, two microphones and a weather station collected sound and meteorological data. The measurements are combined with spatial aircraft radar data for a period of one month. Statistical analyses are conducted to gain insights into the causes of variance in shielding effects.

This paper presents a method to combine and analyse sound, flight and meteorological data, for one-second time intervals. Aircraft orientation, obstruction from buildings between source and receiver, operation type and propulsion type influence the building shielding for this case study. The orientation of airplanes relative to the field lab records the highest effect on the shielding of the analysed variables (R^2=0.58).

*__Corresponding author__: *f.g.e.wuite@tudelft.nl.*
__Copyright__: *©2023 Wuite et al. This is an open-access article distributed under the terms of the Creative Commons Attribution 3.0 Unported License, which permits unrestricted use, distribution, and reproduction in any medium, provided the original author and source are credited.*

Keywords: *Aircraft noise, Urban design, Meteo effects, Modelling*

1. INTRODUCTION

Aircraft noise is a major problem in urban airport regions. Prolonged exposure to noise has adverse effects on health and well-being of people [1]. Long-term exposure to aircraft noise can lead to a variety of negative health impacts, including increased risk of cardiovascular disease, sleep disturbance, and hearing loss.

Dutch aircraft noise contours for building regulations are currently based on computational simulations of noise propagation that assume flat grass surfaces and omit the built environment. This approach overlooks the impact of buildings on noise attenuation and shielding [2]. As a result, building regulations may not accurately represent the noise levels experienced by those living in affected areas.

Sound that travels from aircraft to a receiver on eye-height is affected by both atmospheric refraction and the local spatial context, e.g. surface reflections and edge diffraction around buildings. The sound propagation in urban canyons however depend on a variety of factors, including wind speed and direction [3], building height [4], and orientation [5] to the flight path .

Over the past decades several studies have demonstrated the positive impact of having quiet building sides near dwellings in urban areas. The central idea of a quiet facade is a difference in sound pressure levels (SPL from now on) between facades facing towards a sound source, and facades which are shielded from exposure to sound emanated from the sound source. Despite that various studies focused on quiet sides for buildings near (rail-)

roads, only a few studies have studied the shielding capacity of buildings for aircraft noise.

Nonetheless, potential shielding properties yielded for buildings are mostly studied in relation to highly controlled environments. Conclusions are based on the maximum SPLs, without further analysis on the factors that explain the variance in the data sets.

First conclusions have been drawn by Lugten et al. (2022), recording differences of up to 14.6dB(A) between shielded and non-shielded sides of courtyards [6]. This demonstrates the significant impact that buildings can have on aircraft noise attenuation. However, these differences are only based on the analysis of averaged and maximum SPL, and do not explain the underlying variance between individual flights, or during a single aircraft flyover. By studying the impact of buildings on aircraft noise attenuation with a higher resolution in time, a more complete understanding of the factors that influence building shielding of aircraft noise can be developed. The effect size or interaction effect of single of multiple variables is studied by regression models, or similar statistical methods. The article presents a method of combining the data from multiple sources, and examines which factors contribute to aircraft noise in a street canyon, based on in-situ measurements. This article examines the effects of aircraft position, meteorological variables, and building composition on urban noise levels. The study has two objectives, namely

1. Developing a methodology to combine aircraft radar data, in-situ meteorological data, building geometry data, and SPLs for 1 second intervals.

2. Analysing the influence of local meteorological variables, aircraft positional variables, geometrical building properties, and aircraft operational variables on outdoor sound pressure differences between exposed and shielded courtyard positions.

This article first describes the experimental setup used in the study. Next, the data collected from the experiment is introduced, followed by a description of the processing steps to combine the meteorological, flight path, geometric, and sound data. The analysis of the influence factors is presented in the results section. The article ends with the drawn conclusions and further lines of research.

2. EXPERIMENTAL SETUP

2.1 Field Lab Description

Built from 120 shipping containers, the field lab simulates three full-scale courtyards of 18x30m and 9 meters in height, translating to three-story buildings., The three courtyards differ in geometry, allowing comparisons between them to assess the relative performance between built environment interventions such as building insets and slanted roofs [6]. Based on previous studies, this article focuses on the shielding effect variation in Courtyard 1 [6].

The field lab is situated in Hoofddorp, close to one of the main takeoff and landing strips of Schiphol airport, the Kaagbaan. Aircraft pass the field lab on in a Southwest-Northeast trajectory on the southeast of the field lab at a minimal ground distance of 600m. The longest walls of the courtyard are placed parallel to the flight path, which, in theory, leaves shielded the facades which face away from the flight path.

For Courtyard 1, the shielding effect in this study is quantified as the difference between the recorded SPL for Microphone 4 (Mic 4 from now on) and Microphone 1 (Mic 1 from now on). Mic 4 is situated on the wall exposed to direct sound from the passing aircraft, whereas Mic 1 is shielded by the courtyard geometry and the overhang (see Fig. 1). Both microphones are of NoisePro series class II, located 0.2m from the container walls. They are equipped with a water repelling wind screen, and connected to the electricity grid, with a backup battery in case of power cuts. The microphones house a 4G transmitter, that uploads SPLs and 1/3-octave bands sound exposure levels (1/3OB from now on) every 0.125s to a cloud server provided by Munisense, where the stored data can be downloaded as a time series .csv format.

In addition, four weather stations are deployed in the field lab. The Davis Vantage Pro2 stations measure the local climate at 1.5m height. They are located in the centre of each courtyard, with the fourth being deployed 50m to the southwest of the field lab in a grass field as a reference measurement. For this study, measurements from station 4 are used. These weather stations record averaged meteorological variables in 1 minute intervals, including rainfall, temperature, relative humidity, barometric pressure, wind speed, and wind direction. All stations are solar powered, while recordings form the stations are sent wirelessly to a on-site computer from which records are exported to a cloud server as .csv files.

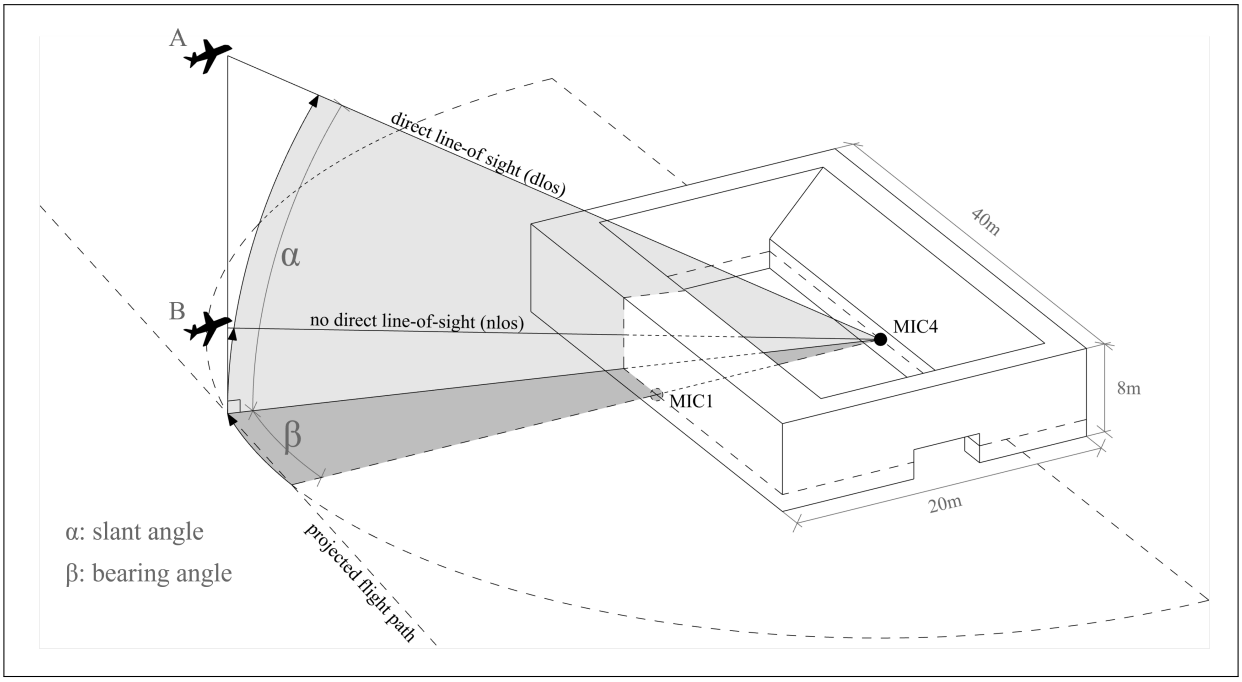


Figure 1. Visualization of courtyard 3, positions of Mic 1 and Mic 4, slant angle α (light grey), bearing β (dark grey), characteristic flight path orientation, and two aircraft positions with direct line-of sight (dlos, A) and no direct line of sight (nlos, B)

2.2 Data sources

The data used in this study can be categorized in to four typologies, namely meteorological data, flight point data, building data, and sound data. Data was collected over the month of February 2023. The following section will elaborate the different types of data sources.

2.2.1 Meteorological data

The meteorological data is sourced from Davis Station 4, located outside of the courtyard. The station is placed in an open field next to the courtyard, at a sufficient distance from the containers. The meteorological data is recorded with a maximum resolution of 1 minute, for which the recorded meteorological variables are averaged. The resulting .csv file provides a time series of rainfall, outdoor temperature, barometric pressure, relative humidity, wind speed, and wind direction for the entire month. A small fraction of the records are missing due to transmission loss between the station and the on-site laptop.

2.2.2 Flight data

The flight point data is sourced from the Schiphol flight tracking portal Casper. All arrivals and departures from the Kaagbaan are included for the month February 2023, accounting to 10681 flights. The data consists of 4D line geodata for each flight, with longitude (x), latitude (y), altitude (z) and timestamp (m) values for each point on the flight trajectory. The flight points are recorded in irregular intervals between 4 and 6 seconds. Each feature carries additional information on the flight number, flight start time, propulsion, operation (arrival/departure), and aircraft type. The dataset is sourced as a .shp Esri shapefile.

2.2.3 Building data

The building data used in the study is a 3D model of the field lab, created in Sketchup. It contains location, orientation, and geometry of the field lab.

2.2.4 Sound data

The sound data consists of a time series of 1-second interval recordings of SPLs recorded by Mic 1 and Mic 4. The data is provided by the portal of Munisense, and consists of a timestamped .csv file. For each microphone, the A-weighted equivalent continuous SPL (LAeq from now on) is recorded. In addition, the equivalent sound exposure level for each 1/3OB is written in the .csv. The data is exported per microphone.

3. METHOD

3.1 Data Processing

To analyse the influence of the causes of variance in building shielding of aircraft noise, the four data sets mentioned in Section 2.2 are processed and subsequently joined by their timestamp. The combined data serves as the base for the analyses. The flowchart in Fig. 2 gives an overview of the processing steps required. The processing steps are run in R using the Rstudio GUI.

The meteorological data is extrapolated to 1s intervals using a na.fill function. As rainfall and heavy winds account for unwanted noise in the sound dataset, timestamps with recorded rainfall and minutes with wind speeds over 17m/s are filtered out.

The flight point data requires pre-processing in Qgis. Using the processing toolbox, the line features are split into flight points, of which x,y,z, and m-values (timestamps) are extracted. The points are filtered by a buffer of 4km around the field lab. The resulting attribute table is exported as a .csv and loaded into Rstudio. There, the timestamps are converted from Unix time differences to a datetime value for later matching. Subsequently, the x,y, and z values are extrapolated to a 1s interval. Relative variables between the field lab are computed, including the ground distance to the field lab, the slant angle (α) of the aircraft, the bearing from field lab to flight point (β), and the and the delay between emission and recording due to the speed of sound. To assure that no instances of multiple flyovers are analysed, only flights are used of which their closest point of passing lies at least 80 seconds apart from the next flight's closest point.

Throughout the flight trajectory, Mic 4 is partially shielded from direct exposure to the sound by the surrounding containers, depending on the position of the flyover relative to the walls surrounding the courtyard (see Fig. 1). The relative position to the field lab can be expressed through a slant angle and bearing angle (see

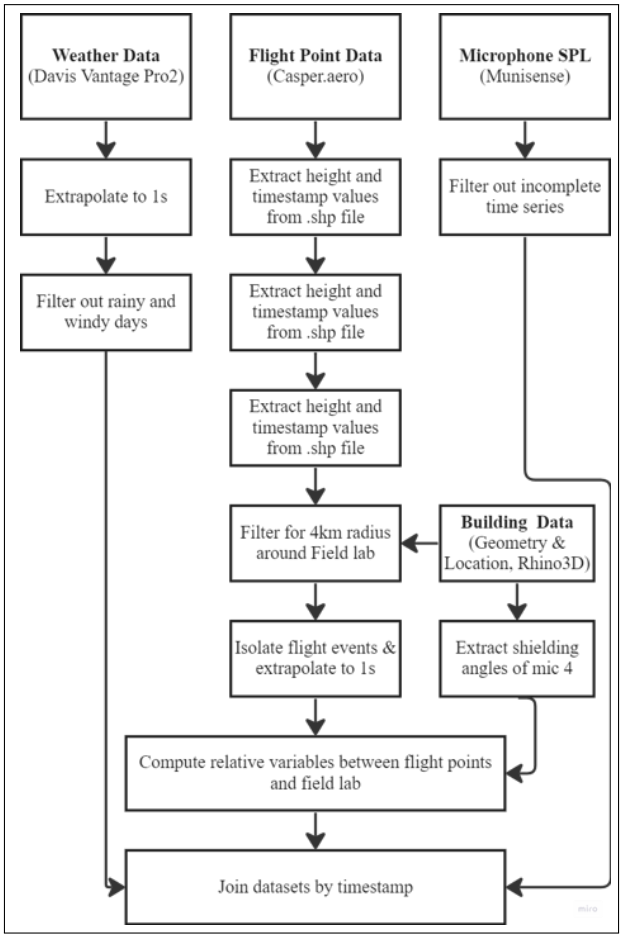


Figure 2. Data sources and processing steps required before analysis

Fig. 1). The slant angle (α) is a function of the ground distance of the flight and its altitude and defined in Eqn. (1). The bearing (β)is the angle between the field lab and the position of an aircraft seen as clockwise from the north. Slant angle and bearing are visualised in Fig. 1) The 3D geomodel is used to determine whether flight points have a direct line of sight (dlos from now on) or no direct line of sight (nlos from now on) to Mic 4 for each position on the path of an aircraft that flies passed the field lab (see Fig. 1). In this article the shielding angle (γ) is defined as the maximum slant angle at which the courtyard walls still shield Mic 4 from a flight point. It is expressed as a function of the bearing angle and courtyard dimensions. For the position of Mic 4, the shielding angle as function of bearing angle is expressed in Eqn. (2). Based on the

shielding angle, a logical column (SHIELDED) is added, describing dlos or nlos between the aircraft and Mic 4.

$$\alpha = \tan^{-1}\left(\frac{z_{flight}}{\sqrt{(x_{FL} - x_{flight})^2 + (y_{FL} - y_{flight})^2}}\right) \quad (1)$$

The acoustical data from Munisense requires a filtering for incomplete records. The two datasets from Mic 1 and Mic 4 are joined to one dataset, and 1/3OB not used for the analysis are removed. Subsequently, for both LAeq and the 1/3OB of 60Hz, 500Hz and 1600Hz, the SPL levels from Mic 1 are subtracted from Mic 4, yielding a difference in SPLs that represents the shielding effect of the courtyard for this study.

After pre-processing of the data sets, they are joined by timestamp. A sound delay is added to the flight point data based on the distance to the field lab. The sound data is joined for timestamps that are available in the flight point data and meteorological data, so that only timestamps with one aircraft in proximity, no rain, and no hard winds are used for the analysis. The resulting data set includes 311097 data points for analyses.

4. RESULTS

From the combined data set, causes of variance in building shielding are determined, listed in Tab. 1. They can be categorized into four groups: Meteorological, building geometry, flight position, and flight operation variables. Their influence is investigated on LAeq and three characteristic 1/3OBs (100Hz, 500Hz, 1600Hz).

4.1 Meteorological Variables

Barometric pressure (R^2=0.1.2e-07, p=0.85) does not show a significant effect on LAeq, outdoor temperature (R^2=0.00015, p¡0.001) and relative humidity (R^2=0.006, p¡0.001) shows a small, but significant effect. A multiple linear regression of wind speed and direction including their interaction effect has a small, but significant effect on LAeq (R^2=0.0085, p¡0.001) . A descriptive visual analysis of the mean LAeq is plotted as a pollution rose from the Openair package [7] (see Fig. 3). A relative increase shielding can be observed for south-eastern wind directions as opposed to north-western wind directions. For south-eastern wind directions, the location of the field lab is downwind compared to the trajectory of the flyovers, which is the opposite for north-western wind directions.

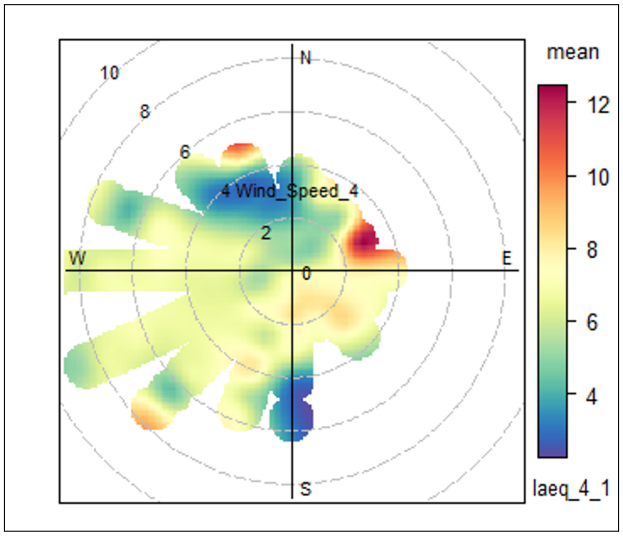


Figure 3. Wind rose of the shielding effect for LAeq, visualizing binned mean shielding effects for wind speeds and directions

4.2 Building Geometry

To include the influence of building geometry on shielding, the microphone differences for dlos and nlos flight points were compared. The difference in courtyard shielding between the two groups is 3.7dB(A), from 9.5dB(A) (dlos) to 5.8dB(A) (see Tab 1). As expected, these differences indicate that the relative shielding of the buildings inside the courtyards decreases if microphone 4 is shielded. Fig. 4 presents density plots of the shielding effect for LAeq and the selected 1/3OBs of the two groups. Density plots apply kernel smoothing over the SPL histogram of all flight points, allowing a visual descriptive analysis of the distribution of SPL levels. For LAeq, a distinct density peak is identified at 13dB(A) for dlos points, while the peak density for nlos points lies at 5dB(A) (Fig. 4, A). For the 100Hz 1/3OB, the differences between dlos and nlos points are comparatively small, the influence of dlos/nlos on shielding effect is comparatively small for 100Hz frequencies (Fig. 4, B). the 500Hz and 1600Hz density curves display similar characteristics as the LAeq curve, the variation of shielding effect increases for 1600Hz relative to 500Hz.

$$\gamma(\beta) = \begin{cases} \beta < 48 | \beta > 228 & NA \\ \beta < 89 | \beta > 187 & \tan^{-1}(\frac{h_{CY} - h_{mic}}{0.5 * y_{CY}} * \frac{|\sin(\beta - 138)|}{180 * \pi}) * 180 * \pi \\ else & \tan^{-1}(\frac{h_{CY} - h_{mic}}{x_{CY}} * \frac{\cos(\beta - 138)}{180 * \pi}) * 180 * \pi \end{cases} \quad (2)$$

Table 1. Variables investigated on their influence on aircraft noise shielding

Variables	Name	Units
Meteorological		
Outdoor Temperature	T_Out	°C
Relative Humidity	RelHum	%
Wind Speed	Wind_Speed	m/s
Wind Direction	Wind_dir	deg
Barometric Pressure	Baro	hPa
Building Geometry		
Shielded	dlos/nlos	logical
Flight position		
Slant Angle		deg
Bearing		deg
ground distance		m
Flight operation		
Aircraft type	ACTYPE	[]
Departure/Arrival	OP	[]
Jet/Propeller	PROPULSION	[]

Table 2. Courtyard shielding for building geometry and flight operation variables

Group	**LAeq**	**100Hz**	500Hz	**1600Hz**
nlos mic 4				
TRUE	5.80	3.63	7.36	4.39
FALSE	9.47	3.15	9.47	9.93
Operation				
D	7.66	3.59	8.45	7.11
A	5.32	2.97	7	3.95
PROPULSION				
Jet	7.15	3.45	8.13	6.42
Turboprop	5.08	2.04	6.24	4.28

4.3 Flight Position and Orientation

The flight position can be expressed as a combination of slant angle, bearing angle, and ground distance. Regression analyses show that ground distance does barely explains variance in LAeq (R=0.057, p¡0.001). A combined linear regression model for LAeq described by bearing and slant angle including their interaction effects yields a Multiple R^2 of 0.58 and p¡0.001. To further investigate distribution of SPLs over bearing and slant angle, a visual analysis is conducted. In Fig. 5, the mean shielding value per spatial bin (consisting of relative bearing angle and slant angle) for all flight points are displayed as a colour gradient for LAeq and 1/3OB. Bearing angles below -40 deg show a lower shielding shielding effect for LAeq, 500Hz, and 1600Hz 1/3OBs. For the 100Hz 1/3OB, the shielding effect is lower than for other frequencies. 500Hz and 1600Hz 1/3OBs show distinct spatial patterns, varying between 4 dB and 16 dB depending on orientation.

4.4 Flight Operation

The flight points are analysed based on three operational variables: operation type (arrival/departure), propulsion type (Jet/Turboprop) and aircraft type. The operation type accounts for difference in group means of 2.4 dB(A). For arrivals, the means shielding effect lies at 5.3 dB(A), whereas for departures it increases to 7.7 dB(A). The courtyards shield jet-powered aircraft (7.2 dB(A)) better than turboprop-powered aircraft (5.1 dB(A)), with a increase in the mean shielding of 2.1 dB(A). The means for the groups are displayed in Tab 2. SPLs do not vary substantially depending on the aircraft type. This is further illustrated by Fig. 6, showing the whisker box plots for the five most prevalent aircraft types in the data set.

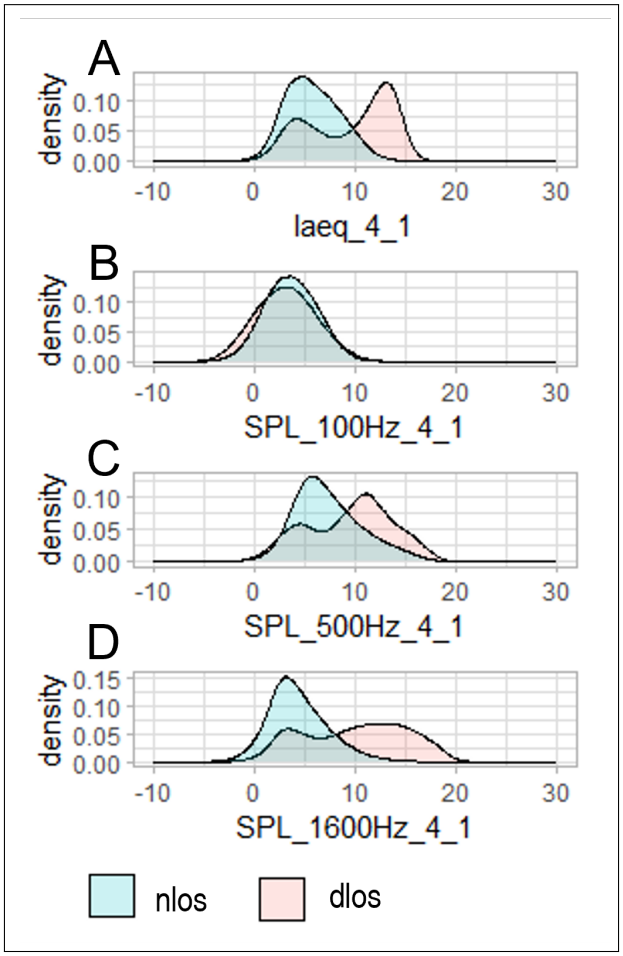


Figure 4. Density curves of SPL differences between Mic 4 and 1 of dlos and nlos flight points for LAeq and characteristic frequencies

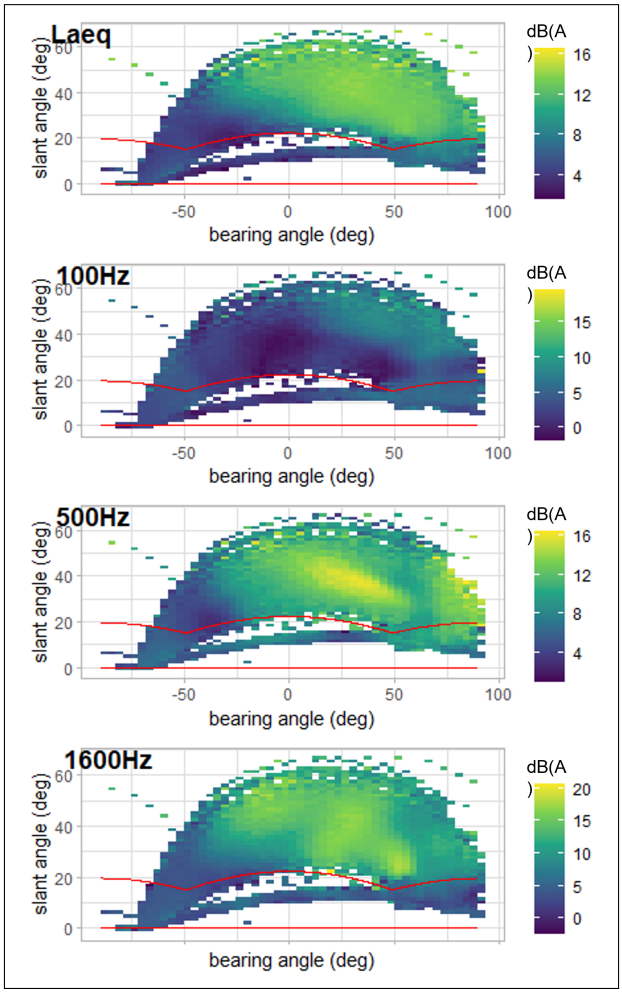


Figure 5. Shielding effect for aircraft orientations relative to field lab for LAeq and characteristic frequencies

5. CONCLUSION

The methodology presented in this study demonstrates a way to combine acoustical data, radar data, geometrical data, and meteorological data at a high temporal resolutions. The aim of the study was to identify underlying relationships between these factors and the level of shielding inside courtyards.

The results in this article describe the variability of aircraft noise shielding by courtyards. Variables that do not have a substantial influence on aircraft noise shielding include outdoor temperature, relative humidity, barometric pressure, ground distance to the aircraft, and aircraft type. The determined factors of influence are direct line of sight to the aircraft from the exposed position, flight orientation ,expressed as the slant angle and bearing, operation type and propulsion type, and wind speed and direction.

The orientation of aircraft relative to the courtyard, depending on altitude and horizontal distance from the courtyards, has a significant effect on the shielding, explaining most variance in the data (R^2=0.58). Due to the direction of the aircraft routes and the decrease of slant angle with increasing ground distance, the density of flight points varies significantly over the orientation. This distribution likely effects the results, the data set will be expanded for multiple months to gain more robust conclu-

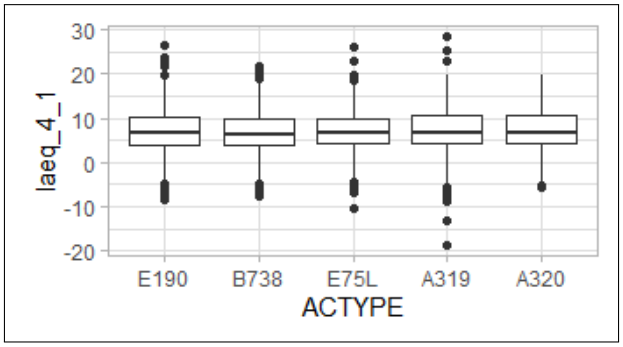


Figure 6. shielding effect box plots for the 5 most occurring aircraft types

sions on the observed distributions.

Courtyard shielding is higher for flight points with dlos (9.5 dB(A)) as compared to nlos (5.8 dB(A)) for LAeq and 1/OBs of 500Hz and higher. For lower frequencies, the courtyard shielding barely differs between dlos and nlos flight points. A secondary density peak for dlos points is observed around 5dB, which is a topic for further investigation in future research.

Wind rose analyses for the influence of wind direction and speed point to a trend of increasing shielding effects for upwind aircraft trajectories (8 dB(A)) as opposed to downwind (5 dB(A)). Whether the runways is used for arrivals or departures depends foremost on wind direction, which will influence the wind rose result.

For operational variables, the courtyards have higher shielding effects for departures (7.7 dB(A)) than for arrivals (5.3 dB(A)). There is also a shielding effect difference of 2 dB(A) between jet (7.2 dB(A)) and Turboprop (5.1 dB(A)) driven aircraft. Further operational variables such as noise classes from the current Dutch aircraft noise model (NRM) could give further insight into shielding effects based on aircraft operation [2].

For this study, the variables of influence are analysed separately. Likely, confounding effects between individual variables exist and will affect the results substantially. An example would be a strong southwestern wind speed, leading to the use of the runway for the Kaagbaan, but also making aircraft climb more steeply, influencing the slant angle and the thrust settings of the aircraft. The confounding between variables is not investigated at this stage, and will be examined in future studies. However, the results gained from the descriptive analyses identify the potential of utilizing a combination of aircraft positional variables, operational variables, dlos and nlos properties between the aircraft and the built environment, and meteorological variables to predict building shielding properties of aircraft noise.

6. ACKNOWLEDGMENTS

The research is funded by the municipality of Haarlemmermeer, the Dutch ministry for Infrastructure and Water Management, the Dutch ministry for housing and domestic affairs, and the Stichting Leefomgeving Schiphol.

7. REFERENCES

[1] A. L. Brown and I. Van Kamp, "Who environmental noise guidelines for the european region: A systematic review of transport noise interventions and their impacts on health," *International journal of environmental research and public health*, vol. 14, no. 8, p. 873, 2017.

[2] H. Van der Wal, P. Vogel, and F. Wubben, "Voorschrift voor de berekening van de lden en lnight geluidbelasting in db (a) ten gevolge van vliegverkeer van en naar de luchthaven schiphol; part 1: Berekeningsvoorschrift," *National Aerospace Laboratory*, 2001.

[3] S. C. Trikootam and M. Hornikx, "The wind effect on sound propagation over urban areas: Experimental approach with an uncontrolled sound source," *Building and environment*, vol. 149, pp. 561–570, 2019.

[4] P. J. Lee and J. Kang, "Effect of height-to-width ratio on the sound propagation in urban streets," *Acta Acustica united with Acustica*, vol. 101, no. 1, pp. 73–87, 2015.

[5] Y. Hao and J. Kang, "Influence of mesoscale urban morphology on the spatial noise attenuation of flyover aircrafts," *Applied Acoustics*, vol. 84, pp. 73–82, 2014.

[6] M. Lugten, "Assessing the influence of street canyon shape on aircraft noise: results from measurements in courtyards near amsterdam schiphol airport," in *51st International Congress and Exposition on Noise Control Engineering, Internoise 2022*, pp. 6474–6485, Institute of Noise Control Engineering, 2022.

[7] D. C. Carslaw and K. Ropkins, "openair — an r package for air quality data analysis," *Environmental Modelling Software*, vol. 27–28, no. 0, pp. 52–61, 2012.